Answer to the comments from Co-Editor

Comments to the Author:

The authors have done a good job in revising this paper. I noticed a few language issues when reading the text. I recommend that before uploading the final text file, the authors go through the text once more to correct the grammar.

As suggested by the Co-Editor the paper was checked in order to correct the grammar. Yellow colour highlights changes made in this new version of the manuscript.

Trends analysis of PM source contributions and chemical tracers in NE Spain during 2004 - 2014: A multi-exponential approach.

Marco Pandolfi [1,], Andrés Alastuey [1], Noemi Pérez [1], Cristina Reche [1], Iria Castro [1], Victor Shatalov [2] and Xavier Querol[1]*

[1] Institute of Environmental Assessment and Water Research, c/ Jordi-Girona 18-26, 08034 Barcelona, Spain

[2] Meteorological Synthesizing Centre – East, 2nd Roshchinsky proezd, 8/5, 115419 Moscow, Russia

**Corresponding author: marco.pandolfi@idaea.csic.es*

Abstract

In this work for the first time data from two twin stations (Barcelona, urban background, and Montseny, regional background), located in NE of Spain, were used to study the trends of the concentrations of different chemical species in PM_{10} and $PM_{2.5}$ along with the trends of the PM_{10} source contributions from Positive Matrix Factorization (PMF) model. Eleven years of chemical data (2004–2014) were used for this study. Trends of both specie concentrations and source contributions were studied using the Mann-Kendall test for linear trends and a new approach based on multi-exponential fit of the data. Despite the fact that different PM fractions ($PM_{2.5}$, PM_{10}) showed linear decreasing trends at both stations, the contributions of specific sources of pollutants and of their chemical tracers showed exponential decreasing trends. The different types of trends observed reflected the different effectiveness and/or time of implementation of the measures taken to reduce the concentrations of atmospheric pollutants. Moreover, the trends of the contributions of specific sources such as those related with industrial activities and with primary energy consumption mirrored the effect of the financial crisis in Spain from 2008. The sources that showed statistically significant downward trends at both Barcelona (BCN) and Montseny (MSY) during 2004-2014 were *Secondary sulfate*, *Secondary nitrate*, and *V-Ni bearing* source. The contributions from these sources decreased exponentially during the considered period indicating that the observed reductions were not gradual and consistent over time. Conversely, the trends were less steep at the end of the period compared to the beginning thus likely indicating the attainment of a lower limit. Moreover, statistically significant decreasing trends were observed for the contributions to PM from the *Industrial/Traffic* source at MSY (mixed metallurgy and road traffic) and from the *Industrial* (metallurgy mainly) source at BCN. These sources were clearly linked with anthropogenic activities and the observed decreasing trends confirmed the effectiveness of pollution control measures implemented at EU or regional/local levels. Conversely, at regional level the contributions from sources mostly linked with natural processes such as *Aged Marine* and *Aged Organic*s did not show statistically significant trends. The trends observed for the PM_{10} source contributions well reflected the trends observed for the chemical tracers of these pollutant sources.

1. Introduction

Meeting the air quality (AQ) standards is one of the major environmental objectives to protect people from breathing air with high levels of pollution. Many studies have been published in these last years showing clearly that the concentrations of particulate matter (PM), and other air pollutants such as sulfur dioxide (SO_2) and carbon monoxide (CO), have markedly decreased during the last 15 years in many European Countries (EEA, 2013; Barmpadimos et al., 2012; Cusack et al., 2012; Querol et al., 2014; Guerreiro et al., 2014 among others). Cusack et al. (2012) reported the reduction in $PM_{2.5}$ concentrations observed at regional background (RB) stations in Spain and across Europe, and, in most cases, the observed reduction was gradual and consistent over time implying the success of cleaner anthropogenic activities. Barmpadimos et al. (2012) have also shown that PM_{10} concentrations decreased at a number of urban background (UB) and rural background stations in five European countries. Henschel et al. (2013) reported the dramatic decrease in SO_2 levels in six European cities which reflected the reduction in sulfur content in fuels, as part of EU legislation, coupled with the shift towards the use of cleaner fuels. EEA (2013) also reported general decreases in NO_2 concentrations even if lower compared to PM. However, Henschel et al. (2015) showed that the NO_x concentrations at traffic sites in many EU cities remained unchanged underlining the need of further regulative measures to meet the air quality standards for this pollutant. In fact an important proportion of the European population lives in areas exceeding the AQ standards for the annual limit value of NO_2, the daily limit value of PM_{10} and the health protection objective of O_3 (EEA, 2013; 2015). PM_{10} and NO_2 are still exceeded mostly in urban areas, and especially at traffic sites (Harrison et al., 2008; Williams and Carslaw, 2011; EEA, 2013; among others). In Spain for example it has been reported that more than 90% of the NO_2 exceedances can be attributed to road traffic emissions (Querol et al., 2012). Guerreiro et al. (2014) furthermore evidenced the notable reduction of ambient air concentration of SO_2, CO and Pb using data available in Airbase (EEA, 2013) covering 38 European countries. Querol et al. (2014) reported trends for 73 measurement sites across Spain including RB, UB, traffic stations (TS) and Industrial sites (IND). They observed marked downward trends for the concentrations of PM_{10}, $PM_{2.5}$, CO and SO_2 at most of the RB, UB, TR and IND sites considered. Similarly, Salvador et al. (2012) detected statistically significant downward trends for the concentrations of SO_2, NO_x, CO and $PM_{2.5}$ at most of the urban and urban-background monitoring sites in the Madrid metropolitan area during 1999-2008. Cusack et al. (2012) and Querol et al. (2014) have also shown the statistically significant decreasing trends for many trace elements (Pb, Cu, Zn, Mn, Cd, As, Sn, V, Ni, Cr) at regional level in NE Spain since 2002.

The observed reduction of air pollutants across Europe is the results of efficient emission abatement strategies as for example those implemented in the Industrial Emission Directives (IPPC Integrated Pollution Prevention and Control and subsequent Industrial Emission Directives 1996/61/EC and 2008/1/EC), the Large Combustion Plants Directive (LCPD; 2001/80/EC), the EURO standards on road traffic emission (1998/69/EC, 2002/80/EC, 2007/715/EC), the IMO (International Maritime Organization) directive on sulfur content in fuel and SO_x and NO_x emissions from ships (IMO, 2011; Directive 2005/33/EC). Additionally, the financial crisis, causing mainly a

reduction of the primary energy consumption from 2008-2009, contributed to the decrease of the ambient concentration of pollutants observed in Spain (Querol et al., 2014).

Moreover, national and regional measures for AQ have been taken in many European Countries. In Spain a national AQ plan was approved in 2011 and updated in 2013 by the Council of Ministers of the Government of Spain. Furthermore, 45 regional and 3 local (city scale) AQ plans have been implemented since 2004 in Spain. These AQ Plans mostly focused on improving AQ at major city centers and specific industrial areas.

Thanks to the aforementioned measures there is clear evidence that the concentrations of PM in many European countries have markedly decreased during the last decades. However, in spite of the above policy efforts, a significant proportion of the urban population in Europe lives in areas exceeding the World Health Organisation (WHO) AQ standards for example for $PM_{2.5}$, PM_{10} and O_3 (EEA, 2013, 2015).

The analysis of the trends of the concentration of air pollutants helps in evaluating the effectiveness of specific AQ measures depending on the pollutant considered. Examining data over time also makes it possible to predict future frequencies and/or rates of occurrence making future projections. For the abovementioned reasons, it is especially attractive the feasibility of studying the trends of the contributions to PM mass from specific pollutant sources along with the trends of the chemical tracers of these sources.

For what we are concerned in the majority of studies dealing with trend analysis linear fits were applied by using Mann-Kendall or Theil-Sen methods (Theil, 1950; Sen, 1968), the latter being available for example in the Openair software (Carslaw, 2012; Carslaw and Ropkins, 2012). However, a linear fit of data does not always properly represent the observed trends. As we will show, different abatement strategies and periods of implementation may change from one pollutant to another thus leading to different trends for different pollutants even over the same period. Thus, non-linear fit of the data may be at times strongly recommended.

The main aim of this work was to study the trends of PM_{10} source contributions and of specific chemical species in both PM_{10} and $PM_{2.5}$ using both the consensus methodology (Mann-Kendall) and the non-linear approach. The data of Spanish national emissions and energy consumption were also evaluated to interpret the observed trends. Understanding past trends may be relevant for devising new strategies for air pollution abatement. PM chemical speciated data collected from 2004 to 2014 at regional (Montseny; NE Spain) and urban (Barcelona, NE Spain) sites were used with this aim. The Positive Matrix Factorization (PMF) model was used to apportion ambient PM_{10} concentrations into pollutant sources. The PMF model, as other Receptor Models (RM), is widely used being a powerful tool to help policy makers to design more targeted approaches to protecting public health. Thus, the novelty of this study lies mainly in a) the opportunity to study the trends of pollutant source contributions from PMF model at two twin stations representative of the urban and regional environments in the Western Mediterranean, and, b) in the use of a novel non-linear approach for trend studies.

2. Measurement sites and Methodology

2.1 Measurement sites

The Montseny measurement station (MSY, 41°46'45.63" N, 02°21'28.92" E, 720 m a.s.l.) is a regional background site in NE of Spain located in a regional natural park about 50 km to the NNE of the city of Barcelona (BCN) and 25 km from the Mediterranean coast (Figure 1). This site is representative of the typical regional background conditions of the Western Mediterranean Basin (WMB) characterized by severe pollution episodes affecting not only the coastal sites closest to the emission sources, but also the more elevated rural and remote areas land inwards (i.e. Pérez et al., 2008; Pey et al., 2010; Pandolfi et al., 2011; 2014). This station is part of the ACTRIS (www.actris.net) and GAW (www.wmo.int/gaw) networks, of the EMEP Program (http://www.emep.int/) and of the measuring network of the Government of Catalonia.

The Barcelona measurement station (BCN, 41°23'24.01" N, 02°06'58.06" E, 68 m a.s.l.) is an urban background measurement site influenced by vehicular emissions from one of the main avenues of the city (Diagonal Avenue) located at a distance of around 300 m (cf. Fig. 1). The BCN measurement site is part of the Air Quality measuring network of the Government of Catalonia. The Metropolitan Area of Barcelona (BMA), with nearly 4.5 million inhabitants, covers an 8 km wide strip between the Mediterranean Sea and the coastal mountain range. Several industrial zones, power plants, and highways are located in the area, making this region one of the most polluted in the WMB (i.e. Querol et al., 2008; Amato et al., 2009; Pandolfi et al., 2012; 2013; 2014). At BCN the location of the measuring station changed in 2009 when it was moved by around 500 m (cf. Fig. 1). The effect of this change on PM measurements performed at BCN will discuss later.

2.2 Real-time and gravimetric PM measurements

Real-time PM concentrations were continuously measured at 1h resolution by optical particle counters (OPC) using GRIMM spectrometers (GRIMM 180 at MSY, and GRIMM 1107, 1129 and 180 at BCN). Hourly PM concentrations were corrected by comparison with 24h gravimetric mass measurements of PM_x (Alastuey et al., 2011).

For gravimetric measurements 24h PMx samples were collected at both stations every 3-4 days on 150 mm quartz micro-fiber filters (Pallflex QAT and Whatman) with a high-volume (Hi-Vol) samplers (DIGITEL DH80 and/or MCV CAV-A/MSb at 30 m^3h^{-1}). The mass of PM_{10} and $PM_{2.5}$ samples collected on filters was determined using the EN 12341 and the EN14907 gravimetric procedures, respectively.

2.2.1 PM chemical speciated data

Once the gravimetric mass was determined from filters, the samples were analyzed with different techniques including acidic digestion (½ of each filter; HNO_3:HF:$HClO_4$), water extraction of soluble anions (¼ of each filter), and thermal-optical analysis (1.5 cm^2 sections). Inductively Coupled Atomic Emission Spectrometry, ICP-AES, (IRIS Advantage TJA Solutions, THERMO) was used for the determination of the major elements (Al, Ca, Fe, K, Na, Mg, S, Ti, P), and Inductively Coupled Plasma Mass Spectrometry, ICP-MS, (X Series II, THERMO) for the trace elements (Li, Ti, V, Cr, Mn, Co, Ni, Cu, Zn, As, Se, Rb, Sr, Cd, Sn, Sb, Ba, rare earths, Pb, Bi, Th, U). Ionic Chromatography was used for the concentrations of NO_3^-, SO_4^{2-} and Cl^-, whereas NH_4^+ was determined using a specific electrode MODEL 710 A+, THERMO Orion. The levels of OC and EC were determined by a thermal-optical carbon analyzer (SUNSET), using protocol EUSAAR_2 (Cavalli et al., 2010). Other analytical details may be found in Querol et al. (2008).

Following the above procedures a total of 1093 PM_{10} and 794 $PM_{2.5}$ filters were collected and analised at MSY during the period 2004-2014. At BCN the collected filters were 1037 and 1063 in PM_{10} and $PM_{2.5}$, respectively.

2.3 Positive Matrix Factorization (PMF) model.

The PMF model (PMFv5.0, EPA) was applied to the collected daily PM_{10} speciated data for source identification and apportionment at both sites. Detailed information about the PMF model can be found in literature (Paatero and Tapper 1994; Paatero 1997; Paatero and Hopke 2003; Paatero et al. 2005). The PMF model is a factor analytical tool reducing the dimension of the input matrix in a limited number of factors (or sources) and it is based on the weighted least-squares method. Thus, most important in PMF applications is the estimation of uncertainties of the chemical species included in the input matrix. In the present study, individual uncertainties and detection limits were calculated as in Escrig et al. (2009) and Amato et al. (2009). Thus, both the analytical uncertainties and the standard deviations of species concentrations in the blank filters were considered in the uncertainties calculations. The signal-to-noise ratio (S/N) was estimated starting from the calculated uncertainties and used as a criteria (S/N >2) for selecting the species used within the PMF model. In order to avoid any bias in the PMF results, the data matrix was uncensored (Paatero 2004). The PMF was run in robust mode (Paatero 1997), and rotational ambiguity was handled by means of the F_{PEAK} parameter (Paatero et al. 2005). The optimal number of sources was selected by inspecting the variation of the objective function *Q* (defined as the ratio between residuals and errors in each data value) with varying number of sources (i.e. Paatero et al., 2002) and by studying the physical meaningfulness of the calculated factors.

2.4 Mann-Kendall (MK) fit

The purpose of the Mann-Kendall (MK) test (Mann 1945, Kendall 1975, Gilbert 1987) is to statistically assess if there is a monotonic upward or downward trend of the variable of interest with time. A monotonic upward (downward) trend means that the variable consistently increases (decreases) through time. The Mann-Kendall test tests the null hypothesis H_0 of no trend, i.e. the observations are randomly ordered in time, against the alternative hypothesis, H_1, where there is an increasing or decreasing monotonic trend. The main advantage of the Mann-Kendall test is that data need not conform to any particular distribution and missing data are allowed. To estimate the slope of the trend the Sen's method was used (Salmi et al. 2002).

2.5 Multi-exponential (ME) fit

A program aiming at studying trends by means of multi-exponential fit of the data was developed within the *The Task Force on Measurements and Modelling* (TFMM) by the *Meteorological Synthesizing Centre – East* (MSC-E; http://www.msceast.org/) group (Shatalov et al., 2015). The TFMM together with the *Task Force on Emission Inventories and Projections* (TFEIP), the *Task Force on Integrated Assessment Modelling* (TFIAM), and *Task Force on Hemispheric Transport of Air Pollution* (TFHTAP) provide a fora for discussion and scientific exchange in support of the EMEP (*European Monitoring and Evaluation Programme*; http://www.emep.int/) work plan which is a scientifically based and policy driven programme under the *Convention on Long-range Transboundary Air Pollution* (CLRTAP; http://www.unece.org/env/lrtap/lrtap_h1.html) to promote the international co-operation and to solve transboundary air pollution problems. The TFMM was established in 2000 to evaluate measurements and modeling and to further develop working methods and tools. In this contest, five EMEP Centers are undertaking efforts in support of the EMEP work plan, namely the *MSC-E*, the *Centre on Emission Inventories and Projections* (CEIP; http://www.ceip.at/), the *Chemical Coordinating Centre* (CCC; http://www.nilu.no/projects/ccc/), the *Meteorological Synthesizing Centre – West* (MSC-W; http://emep.int/mscw/index_mscw.html), and the *Centre for Integrated Assessment Modelling* (CIAM; http://www.iiasa.ac.at/~rains/ciam.html). In 2014 the TFMM initiated a dedicated exercise to assess the efficiency of CLRTAP air pollution mitigation strategies over the past 20 years evaluating the benefit of its main policy instruments. Within this exercise a software was made available by EMEP/MSC-E Center aiming at studying non-linear trends. Annual, monthly and daily resolution data can be analyzed with the help of this program. Since in this paper we will apply the program to annual averages of specie concentrations and source contributions, we restrict the description of the multi-exponential approximations for this case. In particular, seasonal variations are not included into consideration. The basic equations solved by the program for this particular case (annual averages) are reported below:

$$C_t = a_1 \cdot \exp\left(-\frac{t}{\tau_1}\right) + a_2 \cdot \exp\left(-\frac{t}{\tau_2}\right) + \ldots + a_n \cdot \exp\left(-\frac{t}{\tau_n}\right) + \omega_t \quad (1)$$

Where, C_t are the values of the considered time series, with t = 1, …, N, N being the length of the series (years), τ_n are the characteristic times of the considered exponential, a_n are constants and ω_t are the residue values. In the case of single exponential decay (n=1) the characteristic time τ is the time at which the pollutant concentration is reduced to 1/e (= 0.3678) times its initial value. The main difference between linear and exponential fit is that in the latter case the trend is not gradual and constant over time. For an exponential trend the absolute [μg/m^3] reduction per year decreases with time being the highest at the beginning of the period. Conversely, for a linear fit the absolute reduction is constant over time. For an exponential fit, the lower the characteristic time τ the more rapidly the considered quantity vanishes. Deviations from single exponential fit can be taken into account introducing more exponential terms. In this work for example two exponential terms were sometime used. In this case two characteristic times are calculated by the software. If the decrease of the considered quantity is very sharp at the beginning of the period (more than single exponential) than both τ_1 and τ_2 are positive. Conversely, one exponential term with negative τ takes into account for possible increase of the quantity at the end of the period. Both τ_n and a_n are calculated by the program by means of the least square method minimizing the residue ω and the statistically significance of the exponential fit is provided by means of the p-value. The number of exponential terms that should be included into the approximation can be evaluated using F-statistics (i.e. Smith, 2002). For example, the *F*-statistics for the evaluation of the statistical significance of the second term in equation (1) for n = 2 can be calculated as:

$$F = \frac{(SS_1 - SS_2)}{2 \cdot s} \qquad (2)$$

where SS_1 and SS_2 are sums of squares of residual component for approximations with one and two exponential terms, respectively, and s is the estimate of standard deviation of residual component. This statistics follows approximately the Fisher distribution with 2 and N – 2 degrees of freedom. Second exponential is considered to be significant if *F* exceeds the corresponding threshold value at the chosen significance level.

The following parameters can be calculated from equation (1):

- Total Reduction (TR): $$TR = \frac{(C_{beg} - C_{end})}{C_{beg}} = 1 - \frac{C_{end}}{C_{beg}} \qquad (3)$$
- Annual reduction for year *i*: $$R_i = \frac{\Delta C_i}{C_i} = 1 - \frac{C_{i+1}}{C_i} \qquad (4)$$
- Average annual reduction: $$R_{av} = 1 - \left(\frac{C_{end}}{C_{beg}}\right)^{\frac{1}{N-1}} \qquad (5)$$

Where C_{beg} and C_{end} are the first and the last points, respectively, of the exponential fit. The formula for the calculation of the average annual reduction takes into account that the ratio C_i+1 / C_i is a multiplicative quantity, so that geometrical mean of ratios should be used. The relative contribution of residues (Residual Component:

RC) is calculated as the standard deviation of the ratios between the residue values of the fit ω_t (cf. Eq. 1) and the main component of the fit.

The MSC-E also proposed a statistic which measures the deviation of the obtained trend from the linear one (Non-Linearity parameter: *NL*). A trend is defined as linear if the NL parameter is lower than 10%, indicating a small difference between ME and MK fits (Shatalov et al., 2015). In the following, the reported trends were analysed using the MK test for NL<10% and the ME test for NL>10%. More detailed description of the multi-exponential approach is available in the TFMM wiki and in the MSC-E Technical report 2015 (Shatalov et al., 2015).

3. Results

Results are presented and discussed in the following order: In Section 3.1, we compare the trends at both stations of PM_x concentrations from optical counters (OPC; annual data coverage around 90%) and from 24h gravimetric samples (filters; annual data coverage around 20-30%). This comparison will demonstrate the feasibility of studying trends of chemical species concentrations from filters despite the relatively low annual data coverage. In Section 3.2, we compare the magnitude of the trend of $PM_{2.5}$ concentrations at MSY during 2004-2014 (period selected for this study) with the magnitude of trends calculated at the same station over different periods, namely 2002-2010 (the period used in Cusack et al., 2012) and 2002-2014 (representing the largest period of gravimetric $PM_{2.5}$ measurements available at MSY station at the time of writing). This comparison was performed in order to study the differences in the trends over short periods (9 yr to 13 yr). The gravimetric concentrations of $PM_{2.5}$ measured at MSY were used with this aim. Then (Section 3.3), we present and discuss the trends at both stations of chemical species from filters in both PM_{10} and $PM_{2.5}$. In the Section 4.0 we discuss the sources of pollutants identified by PMF model in PM_{10} at both sites. Finally, we present and discuss the trends of PM_{10} source contributions at BCN and MSY (Section 4.1) providing possible explanations for the observed trends. Conclusions are reported in Section 5.

3.1 Trends of PM: Comparison between gravimetric and real-time optical measurements

Annual data coverage is an important factor to take into account in order to study trends of a given parameter. The gravimetric PM measurements, from which chemical speciated data are obtained, are typically performed with rather low frequency over one year. In our case the annual data coverage of gravimetric measurements was around 20-30% at both Barcelona and Montseny. In this section we compare the trends of PM concentrations from gravimetric and real-time optical measurements (Table 1). Given that the trends of the considered PM_x fractions were linear at both sites (NL<10%), only results from MK test were reported in Table 1. However, we will show later (Section 4.1) that the contributions from specific PM_{10} pollutant sources, mainly

those related with anthropogenic activities, showed non-linear (i.e. exponential) decreasing trends thus mirroring the different effectiveness of the mitigation strategies depending on the source of pollutants considered.

As reported in Table 1, statistically significant decreasing trends were observed for the considered PM size fractions at BCN (-2.20 μgm^{-3}/yr with $p<0.001$ for PM_{10} and -1.55 μgm^{-3}/yr with $p<0.01$ for $PM_{2.5}$ from OPC measurements), whereas at Montseny only the $PM_{2.5}$ fraction showed a little significant decreasing trend (-0.26 μgm^{-3}/yr; $p<0.1$ from OPC measurements). Total reductions (TR) ranged between 50.4% (OPC PM_{10} at BCN) to 7.8% (OPC PM_{10} at MSY) and residual component (RC) was lower than 18% reflecting the goodness of the linear (MK) fit used. It must be noted that the higher p-values, magnitude of the trends and TR observed at BCN compared to MSY was likely due to the change of the measuring station in 2009 in BCN (cf. Fig. 1). Based on the comparison between simultaneous PM_x chemical speciated data collected at both BCN measurement sites during 1 month (not shown) we concluded that after 2009 the BCN measuring site was less affected by mineral matter and, to a lesser extent, by road traffic emissions both being important sources of PM in Barcelona. In Figure 1 we highlighted the proximity of the BCN measuring station before 2009 to an unpaved parking and different construction works. The effect of the change of the station in BCN in 2009 on PM_{10} gravimetric measurements was reported in Supporting Information (Figure SI-1). However, despite the change of the station, the comparison between BCN and MSY for specific chemical species and pollutant sources not linked with mineral matter and road traffic emissions was possible.

Table 1 shows that the p-values calculated using gravimetric and OPC measurements were the same despite the different annual data coverage. The differences in the magnitude of the trends were 22% and 24% between gravimetric and OPC PM_{10} and $PM_{2.5}$ measurements, respectively, at BCN and 24% and 21%, respectively, at MSY. Relative differences of total reductions (TR) ranged between 24% between gravimetric and OPC PM_{10} measurements at MSY and 15% for PM_{10} at BCN. Thus, despite the different data coverage the magnitude of the trends and TR calculated from OPC and gravimetric measurements were rather similar. Other PM mass fractions ($PM_{1\text{-}10}$ and $PM_{2.5\text{-}10}$) and PM ratios (PM_1/PM_{10} and $PM_{2.5}/PM_{10}$) at MSY showed non-statistically significant trends.

3.2 Trends of PM: Comparison among different periods

In this study we used the period 2004-2014 for trends analysis given that gravimetric $PM_{2.5}$ measurements at BCN were available since 2004. Conversely, at MSY $PM_{2.5}$ gravimetric measurements started in 2002. Figure 2 shows the trends of $PM_{2.5}$ concentrations at MSY calculated using the MK test for the three different periods. ME test was not used here given that the observed trends were linear (NL<10%). The period 2002-2010 was the period considered in the paper from Cusack et al. (2012) presenting the trends of $PM_{2.5}$ gravimetric mass and chemical species at MSY. The period 2002-2014 is the largest period with $PM_{2.5}$ filter measurements available at

the time of writing. The trend observed at MSY for the $PM_{2.5}$ fraction during 2004-2014 confirmed what already observed by Cusack et al. (2012) at the same station for the period 2002 – 2010. In Cusack et al. (2012) the MK test provided a decreasing trend of around -0.66 μgm^{-3}/yr at 0.01 significance level (TR = 35%). During the periods 2004 – 2014 and 2002 – 2014 decreasing trends of -0.33 μgm^{-3}/yr ($p<0.1$; TR = 26%) and -0.37 μgm^{-3}/yr ($p<0.05$; TR = 31%), respectively, were observed. Thus, a statistically significant trend for $PM_{2.5}$ mass at regional level can be observed even considering different periods thus confirming the effectiveness of mitigation measures together with the effect of the economic crisis in Spain from 2008. However, it should be noted that the statistical significance of the trends observed for the larger periods was lower compared to Cusack et al. (2012). The difference observed in the magnitude of the trends during 2004-2014 compared to the results provided by Cusack et al. (2012) was mainly due to the increase of $PM_{2.5}$ mass concentration in 2012 (cf. Figure 2). Chemical $PM_{2.5}$ speciated data revealed that this increase was partly driven by organic matter showing a mean annual concentration in 2012 higher by around 20% compared to the 2004-2014 average.

3.3 Trends of chemical species

The trends of the annual mean concentrations of chemical species at BCN and MSY are reported in Table 2 (for PM_{10}) and Table 3 (for $PM_{2.5}$). Figure 3 (for BCN) and Figure 4 (for MSY) show the trends of chemical species in PM_{10}. In Tables 2 and 3 and Figures 3 and 4 only the species having statistically significant trends were reported.

As already noted we assume that the change of the station in BCN in 2009 affected the trends of the concentrations of OC, EC, Cu, Sn, Sb and Zn (mainly traffic tracers), Al_2O_3, Ca, Mg, Ti, Rb, Sr (crustal elements related with both natural and anthropogenic sources) and Fe (traffic and crustal tracer). These chemical species at BCN were removed from Tables 2 and 3 and from Figure 3.

Other species measured in BCN were not affected by the change of the station. These are SO_4^{2-}, NH_4^+, V, Ni (related with heavy oil combustion in the study area according to source apportionment results, cf. Par. 4), Pb, Cd, and As (related with industrial/metallurgy activities), Na and Cl (sea spray), and NO_3^-. Although nitrate particles in Barcelona were mainly from traffic, the concentrations of these particles were not strongly affected by the change of the station due to their secondary origin. The MSY station will be considered as reference station given that no location change occurred at this monitoring site during the study period.

Statistically significant exponential trends ($p < 0.01$ or 0.001) were mainly observed for the industrial tracers (Pb, Cd, As) in both PM_{10} and $PM_{2.5}$. For these elements TR was high and around 50-80% in PM_{10} and 67-81% in $PM_{2.5}$. The RCs were lower than 20% thus suggesting the goodness of the exponential fits used to study the trends of these species. Exponential fits were on average needed indicating that the trends were not gradual and consistent over time and that the effectiveness of the control measures for these pollutants was stronger at the beginning of the period under study (2004-2009 approximately) compared to the end of the period (Figs. 3 and 4). This is also evident by comparing the linear MK fit (dashed black line) with the ME fit (red line) in Figs. 3

and 4. In PM_{10} the magnitudes of the trends ranged between -0.00222 μgm^{-3}/yr (Pb; $p<0.001$) to -3.10E-5 μgm^{-3}/yr (Cd; $p<0.001$) at BCN and from -0.00031 μgm^{-3}/yr (Pb; $p<0.01$) to -1.12E-5 μgm^{-3}/yr (Cd; $p<0.01$) at MSY. In $PM_{2.5}$ the magnitude of the trends were similar and ranged between -0.00163 μgm^{-3}/yr (Pb; $p<0.001$) and -3.11E-5 μgm^{-3}/yr (Cd; $p<0.001$) at BCN and between -0.00049 μgm^{-3}/yr (Pb; $p<0.001$) and -1.35E-5 μgm^{-3}/yr (Cd; $p<0.001$) at MSY. Similar magnitude of the trends for these species in both PM fractions at both sites confirmed the common origin of these elements and the impact at regional scale of industrial sources. For Pb and Cd the characteristic time (τ) of the exponential trends was similar at both sites, whereas for As it was higher due to the slightly less intense exponential downward trend observed for As compared to Cd and Pb. Note that the PMF analysis (cf. Section 4) revealed that the concentrations of As were explained by multiple sources (especially at BCN) whereas the *Industrial/metallurgy* source alone explained more than around 70% of Pb and Cd concentrations (not shown). The implementation of the IPPC Directive in 2008 in Spain is the most probable cause for this downward trend. The decrease observed for Pb, Cd and As may be also attributed to a decrease in the emissions from industrial production (smelters, Querol et al., 2007) at a regional scale around Barcelona.

The concentrations of V and Ni in Barcelona in both PM_{10} and $PM_{2.5}$ fractions showed very similar exponential decreasing trends. Similar characteristic times (around 10-11 yr), TR (around 59-63%) and RC (15-17%) in both fractions suggested the common and mainly fine origin of these two elements. At MSY, V and Ni showed linear trends likely because of the higher distance of the MSY station to the sources of V and Ni (shipping and, before 2008, energy production) compared to BCN. Note also that the NL parameter for BCN V and Ni was around 10-12%, indicating that in this case the exponential fit did not differ very much from the linear one. Total reduction for V and Ni at MSY was around 59-64% and 42-43%, respectively, and RCs were lower than 24%.

Sn and Cu in PM_{10} at MSY showed very similar behavior decreasing linearly with time with TR around 36-39% and RC around 16-20%. Decreasing rates of -3.65E-5 μgm^{-3}/yr ($p<0.05$) and -0.00014 μgm^{-3}/yr ($p<0.05$) were observed in PM_{10} for Sn and Cu, respectively. In $PM_{2.5}$, the concentrations of Sn and Cu decreased markedly compared to PM_{10} at the rate of -0.00084 μgm^{-3}/yr ($p<0.001$) and -0.00026 μgm^{-3}/yr ($p<0.01$), respectively. This difference could be explained by possible sources of coarser Sn and Cu which reduced the magnitude of the trends in PM_{10} mass fraction. Sb showed marked decreasing trends in both PM mass fractions compared to Sn and Cu with TR around 62-70%. The magnitude of the trend for Sb was similar in both fractions and around -3.57 ÷ -3.86E-5 μgm^{-3}/yr. The concentrations of Sb were better fitted with exponential curves (SE with $p<0.01$ in PM_{10} and DE with $p<0.01$ in $PM_{2.5}$). The DE fit for Sb in $PM_{2.5}$ had one positive and one negative characteristic time, the latter needed to explain the slight increase in Sb concentrations at the end of the considered period. The marked decreasing trend observed for Sb compared to other traffic tracers could be explained by a progressive reduction of Sb contained in the vehicle brakes. Cr did not show a statistically significant trend in both PM fractions.

Sulfate (SO_4^{2-}) and ammonium (NH_4^+) particles concentrations showed very similar behavior in $PM_{2.5}$ and PM_{10} size fractions due to their fine nature. In BCN the magnitude of the trends were -0.37868 μgm^{-3}/yr ($p<0.001$) and -0.11095 μgm^{-3}/yr ($p<0.001$) for SO_4^{2-} and NH_4^+, respectively, in PM_{10} and -0.32778 μgm^{-3}/yr ($p<0.001$) and -0.12701 μgm^{-3}/yr ($p<0.001$), respectively, in $PM_{2.5}$. The trends were SE with very similar characteristic times (9.64-9.81 yr in PM_{10} and 9.69-10.53 yr in $PM_{2.5}$), TR (64-65% in PM_{10} and 61-64% in $PM_{2.5}$) and RC (12-14% in PM_{10} and 9-15% in $PM_{2.5}$). At MSY the magnitude of the trends of SO_4^{2-} and NH_4^+ and their statistically significance were lower compared to BCN in both fractions. Moreover, at MSY the trends were linear for SO_4^{2-} in both fractions (as for V and Ni). These differences could be explained by the distance of MSY to direct specific sources of sulfate, such as shipping, compared to BCN, thus slightly reducing the magnitude and the statistically significance of the trend of SO_4^{2-} at regional level. It is also interesting to note the similitude between the characteristic times of the exponential fits for V and Ni and SO_4^{2-} in both PM fractions at BCN suggesting the main common origin of these chemical species. Possible reasons for the observed reduction in the concentrations of ambient sulfate in and around Barcelona will be discussed later.

Fine NO_3^- (Table 3) showed statistically significant SE trends similar at both sites with $p<0.001$, TR around 73-82%, RC around 16-21% and characteristic times around 5.8-7.6 yr. In PM_{10} the TR were lower and around 54-64% and the fits were linear at MSY and SE at BCN. The SE fit in PM_{10} at BCN provided a characteristic time around 9.8 yr which was higher compared to the τ obtained for the fine mode (7.6 yr) thus indicating that fine NO_3^- had a more pronounced downward trend compared to PM_{10} NO_3^-.

For the mineral species (Al_2O_3, Ca, Fe) linear (with the exception of Al_2O_3 in $PM_{2.5}$ which was SE) and statistically significant decreasing trends were detected at MSY. On average the TR was higher in the fine fraction, ranging from 50% for Ca to 66% for Al_2O_3, compared to PM_{10} (6-38% cf. Table 2). Downward decreasing trend for crustal material in $PM_{2.5}$ at MSY was also reported by Cusack et al. (2012) for the period 2002 – 2010 and by Querol et al. (2014) for the period 2001 – 2012. These trends were probably driven by weather conditions associated with negative NAO index (iNAO) that could be the cause for this slight reduction observed in crustal material. Pey et al. (2013) found a correlation between iNAO (calculated between June and September) and the contribution of Saharan dust to PM_{10} mass in NE of Spain and showed that the more negative is the iNAO the lower is the dust contribution to PM. The iNAO was unusually negative during the period 2008 – 2012 (http://www.cpc.ncep.noaa.gov/products/precip/CWlink/pna/norm.nao.monthly.b5001.current.ascii) thus likely contributing to explain the observed trends of crustal elements. Moreover, negative NAO can favour the presence of fronts that can sweep the Iberian Peninsula from West to East causing stronger winds and less stagnant conditions thus favouring the dispersion of pollutants. In addition, as suggested by Cusack et al (2012), it could also be hypothesised that some part of the crustal material measured at MSY is a product of the construction industry. The construction industry in Spain has been especially affected by the current economic recession and crustal material produced by this industry may have contributed to the crustal load in $PM_{2.5}$. For example the number of home construction works in Barcelona during 2008 – 2014 (from the beginning of the economic crisis; mean number of works = 1281) reduced by around 75% compared to the period 2000 – 2007;

436 mean number of works = 5187) (http://www.bcn.cat/estadistica/castella/dades/timm/construccio/index.htm).
437 The fact that the total reduction calculated for mineral elements reported in Tables 2 and 3 was higher in $PM_{2.5}$
438 compared to PM_{10} could corroborate the hypothesis of an anthropogenic contribution to the mineral matter
439 measured at MSY.

440 Finally, Na concentrations showed linear decreasing trends at both sites, with the exception of PM_{10} Na at MSY.
441 Other species at MSY such as OC and EC did not show statistically significant trends. Consider that the
442 concentrations of EC at MSY are very low and around at 0.2-0.3 $\mu g/m^3$ as annual mean. Both anthropogenic
443 activity and biomass burning were expected to contribute to this chemical specie. Concerning OC the lack of
444 trend was probably due to the contribution from biogenic sources to the concentration of this specie at regional
445 level.

446

447 **4. PMF source profiles and contributions**

448 Eight and seven sources were detected at BCN and MSY, respectively, in PM_{10} from PMF model. The absolute
449 and relative contributions of these sources to the measured PM_{10} mass were reported in Figure 5 whereas the
450 chemical profiles of the detected sources were reported in Supporting Information (Figure SI-2).

451 Some sources were common at both BCN and MSY. These are: *Secondary Sulfate* (secondary inorganic source
452 traced by SO_4^{2-} and NH_4^+ and contributing 3.95 $\mu g/m^3$ (23.7%) and 4.67 $\mu g/m^3$ (13.7%) at MSY and BCN,
453 respectively), *Secondary nitrate* (secondary inorganic source traced by NO_3^- and NH_4^+ and contributing 1.31
454 $\mu g/m^3$ (7.9%) and 4.45 $\mu g/m^3$ (13.1%) at MSY and BCN, respectively), *V-Ni bearing* source (traced mainly by V, Ni
455 and SO_4^{2-} it represents the direct emissions from heavy oil combustion and contributed 0.71 $\mu g/m^3$ (4.3%) and
456 3.32 $\mu g/m^3$ (9.8%) at MSY and BCN, respectively), *Mineral* (traced by typical crustal elements such as Al, Ca, Ti,
457 Rb, Sr and contributing 2.70 $\mu g/m^3$ (16.2%) and 4.61 $\mu g/m^3$ (13.6%) at MSY and BCN, respectively), *Aged marine*
458 (traced by Na and Cl mainly with contributions from SO_4^{2-} and NO_3^- and contributing 1.76 $\mu g/m^3$ (10.6%) and
459 5.73 $\mu g/m^3$ (16.9%) at MSY and BCN, respectively). Sources detected at MSY but not at BCN were:
460 *Industrial/Traffic* source (traced by EC, OC, Cr, Cu, Zn, As, Cd, Sn, Sb and Pb) which included contributions from
461 anthropogenic sources such as road traffic and metallurgic industries and contributed 1.43 $\mu g/m^3$ (8.6%) and
462 *Aged organics* (traced mainly by OC and EC) with maxima in summer indicating mainly a biogenic origin and
463 contributing 3.78 $\mu g/m^3$ (22.7%). The ratio OC:EC in the *Industrial/Traffic* and *Aged organic* source profiles at
464 MSY were 4.2 and 11.7, respectively, thus indicating a strong influence of aged particles in the latter source with
465 the former source being more fresh. The statistic of the OC:EC ratio based on chemical data at MSY is reported
466 in Supporting Information (Figure SI-3). Mean and median values of OC:EC ratio at MSY were 9.1 and 7.8,
467 respectively.

468 Finally, some sources were detected at BCN but not at MSY: *traffic* (traced mainly by C_{nm}, Cr, Cu, Sb and Fe)
469 contributing 5.14 $\mu g/m^3$ (15.1%), *road/work resuspension* (traced by both crustal elements, mainly Ca, and

traffic tracers such as Sb, Cu and Sn) contributing 4.25 μg/m^3 (12.5%) and *Industrial/metallurgy* (traced by Pb, Cd, As and Zn) contributing 0.96 μg/m^3 (2.8%).

A sensitivity study was performed in order to better interpret the PMF sources at BCN. In fact, for the period 2007 – 2014 separate OC and EC measurements were available and a PMF was performed over this period. The comparison between the PMF source contributions obtained using the period 2007-2014 (separate OC and EC measurements) and the whole period (2004-2014; C_{nm} (non-mineral carbon) available) is reported in Supporting Information (Figure SI-4). As reported in Figure SI-4 the relative differences in source contributions ranged between -3% (*Mineral* source) to +20% (*Industrial* source) and R^2 ranged between 0.894 to 0.997 thus confirming the correct interpretation of the 2004-2014 PMF sources where C_{nm} was used. The OC:EC ratio in the *Traffic* source from 2007-2014 PMF was 1.70 (cf. Figure SI-5) whereas the mean and median OC:EC ratio from chemistry data were 2.5 and 2.3, respectively, thus being in agreement with the contribution of fresh particles from *Traffic* source at BCN.

4.1 Trends of annual PM_{10} source contributions

Figures 6 and 7 and Table 4 show the results from MK or ME test applied to the annual averages of PM_{10} source contributions at BCN and MSY. As already noted we cannot study trends for *Traffic*, *Road/work resuspension* and *Mineral* source contributions at BCN because of the change of the station location in 2009. The contributions that showed statistically significant downward trends at both stations were from *Secondary sulfate*, *Secondary nitrate*, and *V-Ni bearing* sources ($p<0.001$ or $p<0.01$). Moreover, statistically significant decreasing trends were observed for the *Industrial/Traffic* ($p<0.01$) and *Mineral* ($p<0.1$) source contributions at MSY and for the *Industrial/metallurgy* source contribution ($p<0.001$) at BCN. These sources were mostly linked with anthropogenic activities and the observed decreasing trends confirmed the effectiveness of pollution control measures together with the possible effect of the economic crisis in Spain from 2008. Conversely, the contributions from sources mostly linked with natural processes such as *Aged Marine* (at both BCN and MSY) and *Aged Organic* (at MSY) did not show statistically significant trends.

The trends of the *Secondary sulfate* source contributions were DE and SE at BCN and MSY, respectively, thus indicating that the decrease over time of this source contribution was not gradual and monotonic. Overall the observed decreasing trends at both stations may be attributed to the legislation that came into force in 2007-2008 in Spain (the EC Directive on Large Combustion Plants) which resulted in the application of flue gas desulfurization (FGD) systems in a number of large facilities. Figure 8 shows the sharp decreases after 2007 observed for the national SO_2 and NO_x emissions mostly from power generation (MAGRAMA, 2013; Querol et al., 2014). In BCN the two characteristic times (one low and the other high, cf. Table 4) of the DE fit indicated a strong decrease of the *Secondary sulfate* source contribution at the beginning of the period. This decrease was sharper compared to MSY where SE fit was used. This difference was mostly due to the ban of heavy oils and

504 petroleum coke for power generation around Barcelona from 2007. The effects of this AQ Regional Plan were
505 likely more visible in BCN compared to MSY thus explaining the two different exponential fits used. Overall, for
506 the *Secondary sulfate* source contributions the TRs were rather high around 53% at MSY and 67% at BCN with
507 RC ranging from 16% (BCN) to 21% (MSY). The fact that the trend of the *Secondary sulfate* source contribution
508 was exponential likely suggested the attainment of a lower limit and indicated a limited scope for further
509 reduction of SO_2 emissions in our region. In fact, it has been estimated that the maximum in EU will be a further
510 20% reduction through measures in industry, residential and commercial heating and reduced agricultural
511 waste burning (UNECE, 2016). Conversely, in Eastern European countries the scope for reduction is much
512 greater and around 60% (UNECE, 2016).

513 The trends *of the Secondary nitrate* source contributions were SE at both stations with very similar τ (8.96 yr –
514 8.59 yr), TR (67-69 %) and RC (13-17%). The decrease observed for the contribution from the *Secondary Nitrate*
515 source was related to the reduction in ambient NO_x concentrations (Figures 8 and 9). Figure 9 shows the levels
516 of tropospheric NO_2 column from 2005 to 2014 in South Europe from NASA NO_2 OMI level3 plotted using the
517 Giovanni online data system (Acker and Leptoukh, 2007). In Spain it can be observed a general decrease of the
518 concentrations of columnar NO_2 at regional level. Overall, the implementation of European directives affecting
519 industrial and power generation emissions as well as the increase of the proportion of energy produced from
520 renewable sources (cf. Figure 10 for Spain), among others, produced a significant reduction of SO_2 and NO_x
521 emissions. Around Barcelona the observed decreases were also attributed to the decrease of NO_x emissions
522 mainly from the five power generation plants around the city. Moreover, the implementation of the regional
523 AQ Plan for SCRT (continuously regenerating PM traps with selective catalytic reduction for NO_2) and the
524 hybridization and shift to natural gas engines of the Barcelona´s bus fleet may have had an influence in the
525 observed reductions.

526 The decreasing trends ($p<0.01$) of the *V-Ni bearing* source contributions were SE and L at BCN and MSY,
527 respectively, reflecting the trends observed at both stations for the concentrations of V and Ni (cf. Table 2). At
528 BCN the characteristic times (τ) were very similar to the characteristic times calculated for PM_{10} V and Ni (cf.
529 Table 2) which were the main tracers of this source. TRs were around 61% at BCN and 64% at MSY and RCs were
530 similar (19-25 %). The observed decrease in the *V-Ni bearing* source contribution was mainly attributed to the
531 ban of the use of heavy oils and petroleum coke for power generation in Spain from 2008.

532 The *Industrial/Metallurgy* source contribution at BCN decreased exponentially (SE) at the rate of -0.10 μgm^{-3}/yr
533 ($p<0.001$) reflecting the SE decreasing trends observed for the main tracers of this pollutant source (Pb, Cd and
534 As; cf. Table 2). The decrease of industrial emissions was mainly attributed to the implementation of IPPC
535 (Integrated Pollution Prevention and Control) Directives. Moreover, the observed decrease may be attributed to
536 a decrease in the emissions from industrial production (smelters, Querol et al., 2007) at a regional scale around
537 Barcelona. Also, the financial crisis, whose impact on industrial production and use of fuels is evident since
538 October 2008 also contributed to the observed trend. TR and RC for the *Industrial* source contributions at BCN

were 65% and 16%, respectively. As for the contributions from *Secondary sulfate* and *nitrate* sources, the exponential trend observed for the *Industrial/Metallurgy* source contribution suggested the attainment of a lower limit. As evidenced in Fig. 6 the contribution from this source from 2010 was quite low and rather constant.

The contribution of the *Industrial/Traffic* source at MSY showed similar magnitude of the trend (-0.11 μgm^{-3}/yr with $p<0.01$) compared to the BCN *Industrial/Metallurgy* contribution being both sources traced mostly by the same industrial tracers. However, this source at MSY was also traced by traffic tracers (i.e. Cu and Sn) which decreased linearly with time (cf. Table 2), thus likely explaining the linear trend observed for the contribution of this source at MSY. TR and RC were 56% and 13%, respectively, similar to those calculated for *Industrial* source contribution at BCN.

Finally, the *Mineral* source contribution at MSY showed linear little significant decreasing trend ($p<0.1$) in agreement with what observed at the same station by Cusack et al. (2012). As already noted in Section 3.3, this negative trend could be due to both a possible decrease of the emissions of finer anthropogenic mineral species from specific sources such as cement and concrete production and construction works and unusual weather conditions reducing Saharan dust contribution to PM and resuspension of dust.

In order to further interpret the observed trends, annual data on the annual National Energy Consumption (NECo) from different energy sources (MINETUR, 2013) were also evaluated (Figure 10). Overall, the primary energy consumption in Spain (NECo statistical data for Spain-MINETUR, 2013) increased from 2004 to 2007 and decreased from 2007 with marked decrease in 2009. Since 2009, the energy consumption indicator remained rather low and constant until 2012 when an additional decrease in 2013 and 2014 was observed. Oil consumption was fairly constant during 2004–2007 showing an important decrease during 2008–2014. This trend was probably governed by the fuel consumption for traffic road. Coal consumption remained constantly high from 2004 to 2007 whereas, as for the emissions of SO_2 (Fig. 8), a sharp decrease occurred from 2007. However, in the period 2011-2014 there was an important increase of coal consumption leading to an average consumption similar to the year 2008. However, the implementation of FGD systems contributed to maintain SO_2 at low concentrations, even in the coal production regions in Spain (cf. Querol et al., 2014). The hydroelectric generation was rather specular to coal consumption. For example, the increase in 2010 of hydroelectric consumption, due to high rainfall rate, mirrored the decrease in the coal consumption observed the same year. Finally, renewable energy consumption increased by 440% from 2004 to 2014, with a gradual growth in the NECo.

5.0 Conclusions

PM chemical speciated data collected at two twin stations in NE of Spain (Barcelona: urban background station and Montseny: regional background station) during 2004 – 2014 were used to study the trends of the

contributions of pollutant sources from PMF model and of their chemical tracers. Despite the fact the trends of different PM fractions ($PM_{2.5}$ and PM_{10}) were linear during the period under study, the trends of specific chemical elements and source contributions were exponential demonstrating the different effectiveness and/or time of implementation of the different mitigation strategies. Statistically significant exponential trends ($p < 0.01$ or 0.001) were mainly observed for the industrial tracers (Pb, Cd, As) in both PM_{10} and $PM_{2.5}$ and at both sites. The concentrations of V and Ni showed exponential trends in BCN and linear trends at MSY likely because of the higher distance of the MSY station to the sources of V and Ni (shipping and, before 2008, energy production) compared to BCN. Traffic tracers at MSY (Sn, Cu) showed very similar linear decreasing trends with higher magnitude of the trends in the fine ($PM_{2.5}$) fractions compared to PM_{10} likely because of possible sources of coarser Sn and Cu reducing the magnitude of the trends in the PM_{10} mass fraction. The concentrations of Sb at MSY showed marked exponential decreasing trend compared to other traffic tracers (Cu and Sn) which could be explained by a possible progressive reduction of Sb content in vehicle brakes. Secondary inorganic aerosols (SO_4^{2-}, NO_3^- and NH_4^+) also showed marked decreasing trends (both linear and exponential) in both fractions and at both sites. However, in general the magnitude of the trends for these species and their statistical significance were higher at BCN compared to MSY.

The PM_{10} source contributions that showed statistically significant downward trends at both Barcelona (BCN; UB) and Montseny (MSY; RB) were from *Secondary sulfate*, *Secondary nitrate*, and *V-Ni bearing* sources. For these source contributions the decreasing trends were exponential indicating that the trends were not gradual and consistent over time and that the effectiveness of the control measures for these pollutants was stronger at the beginning of the period under study (2004-2009 approximately) compared to the end of the period considered. Statistically significant decreasing trends were observed for the contributions from *Industrial/Traffic* and *Mineral* sources at MSY and from the *Industrial/metallurgy* source at BCN. These sources were mostly linked with anthropogenic activities and the observed decreasing trends confirmed the effectiveness of pollution control measures implemented at EU or regional/local levels. The economic crisis which started in 2008 in Spain also contributed to the observed trends. Conversely, the contributions from sources mostly linked with natural processes such as *Aged Marine* (at both BCN and MSY) and *Aged Organic* (at MSY) did not show statistically significant trends. The general trends observed for the calculated PMF source contributions well reflected the trends observed for the chemical tracers of these pollutant sources. The decrease in the *Secondary sulfate* source contribution was mainly attributed to the EC Directive on Large Combustion Plants implemented in Spain from 2008, resulting in the application of fuels gas desulfurization (FGD) systems in a number of large facilities. Moreover, according to the 2008 Regional AQ Plan, the use of heavy oils and petroleum coke for power generation was forbidden around Barcelona from 2008 in favour of natural gas. As a consequence, a decrease of the contributions from the V-Ni bearing source at both sites was also observed. The decrease observed for the contribution of the *Secondary Nitrate* source was mainly due to the reduction in ambient NO_x concentrations. In Spain a general decrease of the concentrations of NO_2 at regional level was observed and it was mainly related with the lower energy consumption related with the financial crisis. The

609 decrease of nitrates concentrations and *Secondary nitrate* source contributions around Barcelona was also
610 attributed to the decrease of NO_x emissions from the five power generation plants around the city. Moreover, a
611 Regional AQ Plan implementing the SCRT (continuously regenerating PM traps with selective catalytic reduction
612 for NO_2) and the hybridization and shift to natural gas engines of the Barcelona´s bus fleet may have had also an
613 influence in NO_x ambient concentrations. The *Industrial/Metallurgy* source contribution at BCN decreased
614 exponentially reflecting the exponential trends observed for the main tracers of this pollutant source (Pb, Cd
615 and As). The implementation of IPPC (Integrated Pollution Prevention and Control) Directives together with a
616 decrease in the emissions from industrial production (smelters) at a regional scale around Barcelona explained
617 the observed trends. Overall, the magnitude of the decreasing trends of the contributions of the pollutant
618 sources were higher at BCN compared to MSY likely because of the proximity of the BCN measurement site to
619 anthropogenic pollutant sources compared to the MSY site. The results presented in this work clearly confirm
620 the beneficial effect of the AQ measures taken in recent years in Europe. However, the WHO limit values of
621 specific pollutants, PM_{10} and $PM_{2.5}$ among these, are still exceeded especially at urban level and industrial
622 hotspots. To meet the WHO guide levels important actions are still required for the next decade and the
623 interpretation of past air quality trends may yield relevant outcomes for planning further cost-effective actions.
624 We would like to highlight that a non-linear approach to trend studies is very attractive given that some air
625 pollutants reported in this work showed not gradual-with-time reductions. Conversely, for specific pollutant
626 source-contribution/concentration in our region, the decreasing trends were less steep at the end of the period
627 compared to the beginning thus likely indicating the attainment of a lower limit. This was the case for example
628 for the *Secondary sulfate* source contribution decreasing exponentially from 2004 to 2014 thus likely indicating
629 a limited scope for further reduction of SO_2 emissions in our region.

630

631 **Acknowledgments.**

632 This work was supported by the MINECO (Spanish Ministry of Economy and Competitiveness), the MAGRAMA
633 (Spanish Ministry of Agriculture, Food and Environment), the Generalitat de Catalunya (AGAUR 2014 SGR33 and
634 the DGQA) and FEDER funds under the PRISMA project (CGL2012-39623- C02/00). The research leading to these
635 results has received funding from the European Union's Horizon 2020 research and innovation programme
636 under grant agreement No 654109 and previously from the European Union Seventh Framework Programme
637 (FP7/2007-2013) under grant agreement n° 262254. Marco Pandolfi is funded by a Ramón y Cajal Fellowship
638 (RYC-2013-14036) awarded by the Spanish Ministry of Economy and Competitiveness. NO_2 map analyses and
639 visualizations used in this paper were produced with the Giovanni online data system, developed and
640 maintained by the NASA GES DISC. The authors would like to express their gratitude to D. C. Carslaw and K.
641 Ropkins for providing the Openair software used in this paper (Carslaw and Ropkins, 2012; Carslaw, 2012).
642

643

644 **Bibliography**

645 Acker, J. G. and Leptoukh, G.: *Online Analysis Enhances Use of NASA Earth Science Data*, Eos, Trans. AGU, 88, 2,
646 14-17, 2007.

647 Alastuey, A., Minguillón, M.C., Pérez, N., Querol, X., Viana, M. and de Leeuw, F.: *PM10 Measurement Methods*
648 *and Correction Factors: 2009 Status Report*, ETC/ACM Technical Paper 2011/21, 2011.

649 Amato, F., M. Pandolfi, A. Escrig, X. Querol, A. Alastuey, J. Pey, N. Perez, P.K. Hopke, *Quantifying road dust*
650 *resuspension in urban environment by Multilinear Engine: A comparison with PMF2*, Atmos. Environ., 43 - 17,
651 pp. 2770 - 2780. 06/2009, 2009.

652 Barmpadimos, I., Keller, J., Oderbolz, D., Hueglin, C., Prevot, A.S.H.: *One decade of parallel fine ($PM_{2.5}$) and*
653 *coarse (PM_{10}–$PM_{2.5}$) particulate matter measurements in Europe: trends and variability*, Atmos. Chem. Phys., 12,
654 3189–3203, http://dx.doi.org/10.5194/acp-12-3189-2012, 2012

655 Carslaw, D.C., *The OpenAir manual — open-source tools for analysing air pollution data*, Manual for version 0.5-
656 16, King's College, London, 2012.

657 Carslaw, D.C., Ropkins, K.: *OpenAir — an R package for air quality data analysis,* Environ. Model Softw., 27–28,
658 52–61, 2012

659 Cavalli, F., Viana, M., Yttri, K. E., Genberg, J., and Putaud, J.-P.: Toward a standardised thermal-optical protocol
660 for measuring atmospheric organic and elemental carbon: the EUSAAR protocol, Atmos. Meas. Tech., 3, 79-89,
661 doi:10.5194/amt-3-79-2010, 2010.

662 Cusack, M., Alastuey, A., Perez, N., Pey, J., Querol, X.: *Trends of particulate matter (PM2.5) and chemical*
663 *composition at a regional background site in the Western Mediterranean over the last nine years (2002–2010)*,
664 Atmos. Chem. Phys., 12, 8341–8357 http://dx.doi.org/10.5194/acp-12-8341-2012, 2012.

665 EEA: European Environmental Agency Air quality in Europe — 2013 report, EEA report 9/2013, Copenhagen,
666 1725-9177, [107 pp. http://www.eea.europa.eu/publications/air-quality-in-europe-2013], 2013.

667 EEA: European Environmental Agency Air quality in Europe — 2015 report, *Many Europeans still exposed to*
668 *harmful air pollution. Air pollution is the single largest environmental health risk in Europe*, EEA report 11/2015,
669 Copenhagen, 1-7, [http://www.eea.europa.eu/media/newsreleases/many-europeans-still-exposed-to-air-
670 pollution-2015], 2015.

671 Escrig, A., Monfort, E., Celades, I., Querol, X., Amato, F., Min guillon, M. C., and Hopke, P. K.: Application of
672 optimally scaled target factor analysis for assessing source contribution of ambi ent PM10, J. Air Waste
673 Manage., 59(11), 1296–1307, 2009.

674 Gilbert, R.O.: Statistical Methods for Environmental Pollution Monitoring, Wiley, NY, 1987.

675 Guerreiro, C., Leeuw, F. de, Foltescu, V., Horálek, J., & European Environment Agency: *Air quality in Europe 2014*
676 *report*, Luxembourg: Publications Office.
677 http://bookshop.europa.eu/uri?target=EUB:NOTICE:THAL14005:EN:HTML, 2014

678 Harrison, R.M., Stedman, J., Derwent, D.: *New directions: why are PM10 concentrations in Europe not falling?*,
679 Atmos. Environ., 42, 603–606, 2008.

680 Henschel, S., Querol, X., Atkinson, R., Pandolfi, M., Zeca, A., Le Tertre, A., Analitis, A., Katsouyanni, K., Chanel,
681 O., Pascal, M., Bouland, C., Haluza, D., Medina, S., Goodman, P.G.: *Ambient air SO2 patterns in 6 European*
682 *cities*, Atmos. Environ., 79, 236 - 247. 11/2013, 2013.

683 Henschel, S., Le Tertre, A., Atkinson, R.W., Querol, X., Pandolfi, M., Zeka, A., Haluza, D., Antonis, A., Katsouyanni,
684 K., Bouland, C., Pascal, M., Medina, S., Goodman, P.G.: *Trends of nitrogen oxides in ambient air in nine European*
685 *cities between 1999 and 2010*, Atmos. Environ., 117, 234 - 241. 09/2015, 2015.

686 Kendall, M.G.: Rank Correlation Methods, 4th edition, Charles Griffin, London, 1975.

687 MAGRAMA. Inventario Nacional de Emisiones de Contaminantes a la Atmósfera. Ministerio de Agricultura,
688 Alimentación y Medio Ambiente del Gobierno de España. http://www.magrama.gob.es/ca/calidad-y-
689 evaluacion-ambiental/temas/sistemaespanol-de-inventario-sei-/, 2013.

690 Mann, H.B.: Non-parametric tests against trend, Econometrica 13:163-171, 1945.

691 MINETUR. Ministerio de Industria, Energía y Turismo. Gobierno de España: energy statistics and balances.
692 http://www.minetur.gob.es/energia/balances/Balances/Paginas/CoyunturaTrimestral.aspx, 2013.

693 Paatero, P. and Tapper, U.: *Positive Matrix Factorization: a non negative factor model with optimal utilization of*
694 *error estimates of data values*, Environmetrics, 5, 111–126, 1994.

695 Paatero, P.: *Least squares formulation of robust non-negative factor analysis*, Chemometr. Intell. Lab., 37, 23–
696 35, 1997.

697 Paatero, P., Hopke, P. K., Song, X., and Ramadan, Z.: *Understanding and controlling rotations in factor analytic*
698 *models*, Chemometr. Intell. Lab., 60(1–2), 253–264, 2002.

699 Paatero, P. and Hopke, P. K.: *Discarding or downweighting high noise variables in factor analytic models*, Anal.
700 Chim. Acta, 490, 277–289, doi:10.1016/s0003-2670(02)01643-4, 2003.

701 Paatero P.: User's guide for positive matrix factorization programs PMF2 and PMF3, Part1: tutorial. University of
702 Helsinki, Helsinki, Finland, 2004.

703

704 Paatero, P., Hopke, P. K., Begum, B. A., and Biswas, S. K.: *A graphical diagnostic method for assessing the*

rotation in factor analytical models of atmospheric pollution, Atmos. Environ., 39, 193–201, doi:10.1016/j.atmosenv.2004.08.018, 2005.

Pandolfi, M., Cusack, M., Alastuey, a. and Querol, X.: Variability of aerosol optical properties in the Western Mediterranean Basin, Atmos. Chem. Phys., 11(15), 8189–8203, doi:10.5194/acp-11-8189-2011, 2011.

Pandolfi, M., F. Amato, C. Reche, A. Alastuey, R. P. Otjes, M. J. Blom, X. Querol, *Summer ammonia measurements in a densely populated Mediterranean city*, Atmos. Chem. Phys., 12, pp. 7557 - 7575. 08/2012, 2012.

Pandolfi, M., G. Martucci, X. Querol, A. Alastuey, F. Wilsenack, S. Frey, C.D. O'Dowd, M. Dall'Osto, *Continuous atmospheric boundary layer observations in the coastal urban area of Barcelona during SAPUSS*, Atmos. Chem. Phys., 13 - 9, pp. 4983 - 4996. 05/2013, 2013.

Pandolfi, M., Querol, X., Alastuey, A., Jimenez, J. L., Jorba, O., Day, D., Ortega, A., Cubison, M. J., Comerón, A., Sicard, M., Mohr, C., Prévôt, A. S. H., Minguillón, M. C., Pey, J., Baldasano, J. M., Burkhart, J. F., Seco, R., Peñuelas, J., van Drooge, B. L., Artiñano, B., Di Marco, C., Nemitz, E., Schallhart, S., Metzger, A., Hansel, A., Lorente, J., Ng, S., Jayne, J. and Szidat, S.: Effects of sources and meteorology on particulate matter in the Western Mediterranean Basin: An overview of the DAURE campaign, J. Geophys. Res. Atmos., 119(8), 4978–5010, doi:10.1002/2013JD021079, 2014.

Pérez, N., Pey, J., Castillo, S., Viana, M., Alastuey, A. and Querol, X.: Interpretation of the variability of levels of regional background aerosols in the Western Mediterranean, Sci. Total Environ., 407(1), 527–540, doi:10.1016/j.scitotenv.2008.09.006, 2008.

Pey, J., Pérez, N., Querol, X., Alastuey, A., Cusack, M. and Reche, C.: Intense winter atmospheric pollution episodes affecting the Western Mediterranean., Sci. Total Environ., 408(8), 1951–9, doi:10.1016/j.scitotenv.2010.01.052, 2010.

Pey, J., Querol, X., Alastuey, A., Forastiere, F., and Stafoggia, M.: African dust outbreaks over the Mediterranean Basin during 2001–2011: PM10 concentrations, phenomenology and trends, and its relation with synoptic and mesoscale meteorology, Atmos. Chem. Phys., 13, 1395-1410, doi:10.5194/acp-13-1395-2013, 2013.

Querol, X., Viana, M., Alastuey, A., Amato, F., Moreno, T., Castillo, S., Pey, J., de la Rosa, J., Artíñano, B., Salvador, P., García Dos Santos, S., Fernández-Patier, R., Moreno-Grau, S., Negral, L., Minguillón, M.C., Monfort, E., Gil, J.I., Inza, A., Ortega, L.A., Santamaría, J.M., Zabalza, J.: Source origin of trace elements in PM from regional background, urban and industrial sites of Spain, Atmos. Environ., 41, 7219-7231, 2007.

Querol, X., Alastuey, A., Moreno, T., Viana, M.M., Castillo, S., Pey, J., Rodríguez, S., Artiñano, B., Salvador, P., Sánchez, M., Garcia Dos Santos, S., Herce Garraleta, M.D., Fernandez-Patier, R., Moreno-Grau, S., Negral, L., Minguillón, M.C., Monfort, E., Sanz, M.J., Palomo-Marín, R., Pinilla-Gil, E., Cuevas, E., de la Rosa, J., Sánchez de la

737 Campa, A.: *Spatial and temporal variations inairborne particulate matter (PM10 and PM2.5) across Spain 1999–*
738 *2005*, Atmos. Environ., 42, 3694–3979, 2008.

739 Querol, X., M. Viana, T. Moreno, A. Alastuey, J. Pey, F. Amato, M. Pandolfi, et al., *Scientific bases for a National*
740 *Air Quality Plan* (in Spanish), Colección Informes CSIC, 978-84-00-09475-1, 3, 2012.

741 Querol, X., , Alastuey, A., Pandolfi, M., Reche, C., Pérez, N., Minguillón, M.C., Moreno, T., Viana, M., Escudero,
742 M., Orio, A., Pallarés, M., Reina, F.: *2001–2012 trends on air quality in Spain*, Sci. Total Environ., 490, 957–969,
743 doi:10.1016/j.scitotenv.2014.05.074, 2014

744 Salmi, T., Maata, A., Antilla, P., Ruoho-Airola, T., Amnell, T.: Detecting trends of annual values of atmospheric
745 pollutants by the Mann Kendall test and Sen's slope estimates – the Excel template application Makesens,
746 Finnish Meteorological Institute, Helsinki, Finland, 35 pp, 2002.

747 Salvador P., Artíñano B., Viana M., Alastuey A., Querol X.: *Evaluation of the changes in the Madrid metropolitan*
748 *area influencing air quality: analysis of 1999-2008 temporal trend of Particulate Matter*, Atmos. Environ., 57,
749 175-185, 2012.
750

751 Sen, P.K., *Estimates of regression coefficient based on Kendall's tau*, J. Am. Stat. Assoc., 63, 1379–1389, 1968

752 Shatalov V., Ilyin I., Gusev A., Rozovskaya O., Travnikov O.: *Heavy Metals and Persistent Organic Pollutants:*
753 *development of multi-scale modeling and trend analysis methodology.* EMEP/MSC-E Technical report 1/2015,
754 2015.

755 Smith, D.M.: *Computing single parameter transformations*, Communications in Statistics - Simulation and
756 Computation, 32, 605-618, 2002.

757 Theil, H.: *A rank invariant method of linear and polynomial regression analysis, I, II, III,* Proceedings of the
758 Koninklijke Nederlandse Akademie Wetenschappen, SeriesA — Mathematical Sciences, 386–392, 521–525,
759 1397–1412, 1950.

760 UNECE: Towards Cleaner Air. Scientific Assessment Report. EMEP Steering Body and Working Group on Effects
761 of the Convention on Long-Range Transboundary Air Pollution, Oslo. xx+50pp, Eds. Maas, R., P. Grennfelt,
762 www.unece.org/environmental-policy/conventions/envlrtapwelcome/publications.html, 2016.

763 Williams, M.L., D. Carslaw, *New directions: science and policy — out of step on NOx and NO2?,* Atmos. Environ.,
764 45, 3911–3912, 2011.

765

766

Table 1: Trends of different PM mass fractions from gravimetry (grav) and optical (OPC) measurements at BCN (bold italic) and MSY (2004-2014). TR (%) = Total Reduction; RC (%) = Residual Component. Significance of the trends following the Mann-Kendall test: *** (p-value < 0.001), ** (p-value < 0.01), * (p-value < 0.05), + (p-value < 0.1).

PM_x	**PM_x**		**Mann-Kendall fit**			
Fraction	Conc. 2004 (μgm^{-3})	Conc. 2014 (μgm^{-3})	p-value	Trend [μgm^{-3}/yr]	TR [%]	RC [%]
PM_{10} (grav.)	***41.1***	***19.2***	***	***-2.83***	***59.2***	***8.5***
	19.2	13.9		-0.17	10.5	17.6
$PM_{2.5}$ (grav.)	***31.6***	***13.2***	***	***-2.03***	***60.1***	***7.9***
	16.2	9.8	+	-0.33	25.6	17.3
PM_{10} (OPC)	***39.1***	***19.8***	***	***-2.20***	***50.4***	***10.0***
	18.6	12.3		-0.13	7.8	16.9
$PM_{2.5}$ (OPC)	***27.1***	***12.9***	**	***-1.55***	***49.6***	***9.8***
	16.5	9.3	+	-0.26	21.2	17.5

Table 2: Mann-Kendall and Multi-exponential trends of different chemical species in PM_{10} at BCN (bold italic) and MSY. Type of trend: linear (L), single-exponential (SE), double exponential (DE); **a** (μgm^{-3}) and τ (yr) are the constants and the characteristic times, respectively, of the exponential data fittings; NL (%) = Non-Linearity; TR (%) = Total Reduction; RC (%) = Residual Component; ns = not statistically significant; ni = not included. Significance of the trends: *** (p-value < 0.001), ** (p-value < 0.01), * (p-value < 0.05), + (p-value < 0.1).

	PM_{10} (*BCN*;MSY)					**Mann-Kendall fit**	**Multi-exponential fit**				
Specie	Concentration 2004 (μgm^{-3})	Concentration 2014 (μgm^{-3})	Fit type	NL (%)	p-value	Trend [μgm^{-3}/yr]	a (μgm^{-3})	τ (yr)	Trend [μgm^{-3}/yr]	TR (%)	RC (%)
Pb	***0.02685***	***0.00694***	***SE***	***27***	***		***0.03246***	***6.12***	***- 0.00222***	***80***	***17***
	0.00481	0.00190	SE	11	**		0.00553	10.22	-0.00031	62	13
Cd	***0.00043***	***0.00015***	***SE***	***19***	***		***0.00048***	***7.59***	***-3.10e-5***	***73***	***17***
	0.00017	0.00006	SE	18	**		0.00018	7.92	-1.12E-5	72	16
As	***0.00094***	***0.00036***	***SE***	***14***	*****		***0.00118***	***9.11***	***-7.07E-5***	***67***	***11***
	0.00029	0.00017	L	<10	***	-1.29E-5				50	9
V	***0.01116***	***0.00454***	***SE***	***12***	*****		***0.01502***	***10.04***	***-0.00086***	***63***	***17***
	0.00328	0.00175	L	<10	**	-0.00022				59	15
Ni	***0.00531***	***0.00284***	***SE***	***11***	*****		***0.00678***	***10.61***	***-0.00037***	***61***	***16***
	0.00155	0.00100	L	<10	**	-7.10E-5				43	20
Sn	***ni***	***ni***									
	0.00127	0.00057	L	<10	*	-3.65E-5				39	16
Cu	***ni***	***ni***									
	0.00420	0.00216	L	<10	*	-0.00014				36	20
Sb	***ni***	***ni***									
	0.00058	0.00025	SE	11	**		0.00064	10.46	-3.57E-5	62	13
SO_4^{2-}	***5.74436***	***2.28596***	***SE***	***12***	*****		***6.56033***	***9.81***	***-0.37868***	***64***	***12***
	2.84849	1.67712	L	<10	**	-0.11836				42	18
NO_3^-	***5.07816***	***1.72401***	***SE***	***12***	*****		***6.49890***	***9.83***	***-0.37484***	***64***	***15***
	1.80724	0.67419	L	<10	**	-0.10593				54	13
NH_4^+	***1.92062***	***0.57008***	***SE***	***12***	*****		***1.90645***	***9.64***	***-0.11095***	***65***	***14***
	1.14268	0.40135	SE	13	*		1.28868	9.26	-0.07640	66	22
Al_2O_3	***ni***	***ni***									
	0.72357	0.46382	L	<10	*	-0.02383				34	18
Ca	***ni***	***ni***									
	0.42703	0.28279	L	<10	*	-0.01638				38	17
Fe	***ni***	***ni***									
	0.22371	0.14895	L	<10	+	-0.00593				6	44
Na	***1.02188***	***0.77408***	***L***	***<10***	*****	***-0.03943***				***34***	***12***
					ns						

Table 3: Mann-Kendall and Multi-exponential trends of different chemical species in $PM_{2.5}$ at BCN (bold italic) and MSY. Type of trend: linear (L), single-exponential (SE), double exponential (DE); **a** (μgm^{-3}) and τ (yr) are the constants and the characteristic times, respectively, of the exponential data fittings; NL (%) = Non-Linearity; TR (%) = Total Reduction; RC (%) = Residual Component; ns = not statistically significant; ni = not included. Significance of the trends: *** (p-value < 0.001), ** (p-value < 0.01), * (p-value < 0.05), + (p-value < 0.1).

	$PM_{2.5}$ (***BCN***;MSY)					**Mann-Kendall fit**	**Multi-exponential fit**				
Specie	Concentration 2004 (μgm^{-3})	Concentration 2014 (μgm^{-3})	Fit type	NL (%)	p-value	Trend [μgm^{-3}/yr]	a (μgm^{-3})	τ (yr)	Trend [μgm^{-3}/yr]	TR (%)	RC (%)
Pb	***0.02117***	***0.00500***	***SE***	***27***	*****		***0.02390***	***6.24***	***-0.00163***	***80***	***13***
	0.00642	0.00149	SE	28	***		0.00716	6.08	-0.00049	81	18
Cd	***0.00041***	***0.00011***	***SE***	***23***	*****		***0.00047***	***6.81***	***-3.11E-5***	***77***	***13***
	0.00020	0.00005	SE	23	***		0.00020	6.77	-1.35E-5	77	18
As	***0.00069***	***0.00027***	***SE***	***14***	*****		***0.00091***	***9.00***	***-5.43E-5***	***67***	***11***
	0.00029	0.00013	SE	15	**		0.00033	8.56	-2.04E-5	69	19
V	***0.00823***	***0.00368***	***SE***	***11***	*****		***0.01121***	***11.13***	***-0.00061***	***59***	***16***
	0.00271	0.00130	L	<10	**	-0.00017				64	24
Ni	***0.00402***	***0.00185***	***SE***	***10***	*****		***0.00498***	***11.23***	***-0.00027***	***59***	***15***
	0.00189	0.00080	SE	13	**		0.00205	9.36	-0.00012	42	21
Sn	***ni***	***ni***									
	0.00157	0.00043	L	<10	***	-0.00084				61	12
Cu	***ni***	***ni***									
	0.00394	0.00113	SE	14	**		0.00426	8.99	-0.00026	67	13
Sb	***ni***	***ni***									
	0.00053	0.00015	DE	48	**		0.00069 1.3E-6	4.52 -2.50	-3.86E-5	70	16
SO_4^{2-}	***4.86564***	***1.92388***	***SE***	***12***	*****		***5.64582***	***9.69***	***-0.32778***	***64***	***9***
	2.98922	1.43381	L	<10	**	-0.16222				54	15
NO_3^-	***3.45513***	***0.86002***	***SE***	***19***	*****		***4.14459***	***7.61***	***-0.26753***	***73***	***16***
	1.66095	0.29452	SE	30	***		1.96014	5.81	-0.13550	82	21
NH_4^+	***2.19735***	***0.68393***	***SE***	***11***	*****		***2.27813***	***10.53***	***-0.12701***	***61***	***15***
	1.39366	0.48049	SE	18	**		1.62588	7.94	-0.10266	72	14
Al_2O_3	***ni***	***ni***									
	0.30245	0.10153	SE	13	*		0.26678	9.36	-0.01574	66	35
Ca	***ni***	***ni***									
	0.11478	0.06540	L	<10	+	-0.00494				50	33
Fe	***ni***	***ni***									
	0.09679	0.03716	L	<10	*	-0.00504				61	31
Na	***0.27476***	***0.17863***	***L***	<10	***+***	***-0.01247***				***41***	***15***
	0.13091	0.07252	L	<10	*	-0.00584				45	18

Table 4: Mann-Kendall and Multi-exponential trends of source contributions in PM_{10} from PMF at BCN (bold italic) and MSY. Type: linear (L), single-exponential (SE), double exponential (DE); **a** (μgm^{-3}) and τ (yr) are the constants and the characteristic times, respectively, of the exponential data fittings; NL (%) = Non-Linearity; TR (%) = Total Reduction; RC (%) = Residual Component; ni = not included . Significance of the trends following the Mann-Kendall test: *** (p-value < 0.001), ** (p-value < 0.01), * (p-value < 0.05), + (p-value < 0.1).

	PM_{10} (***BCN***;MSY)					**Mann-Kendall fit**	**Multi-exponential fit**				
Source	Contribution 2004 (μgm^{-3})	Contribution 2014 (μgm^{-3})	Fit type	NL (%)	p-value	Trend [μgm^{-3}/yr]	a (μgm^{-3})	τ (yr)	Trend [μgm^{-3}/yr]	TR (%)	RC (%)
Secondary *sulfate*	***10.27***	***3.38***	***DE***	***45***	*****		***12.33*** ***3.82***	***1.65*** ***105.80***	***-0.71***	***67***	***16***
	6.57	3.07	SE	12	**		5.99	13.22	-0.32	53	21
Secondary *nitrate*	***6.99***	***1.96***	***SE***	***14***	*****		***8.54***	***8.96***	***-0.51***	***67***	***13***
	2.03	0.47	SE	15	**		2.44	8.59	-0.15	69	17
V-Ni bearing	***4.23***	***1.84***	***SE***	***11***	*****		***5.66***	***10.59***	***-0.32***	***61***	***19***
	0.79	0.44	L	8	**	-0.07				64	25
Industrial/Metallurgy (BCN)	***1.64***	***0.71***	***SE***	***21***	*****		***1.76***	***9.56***	***-0.10***	***65***	***16***
Mineral	***ni***	***ni***									
	3.46	2.32	L	5	+	-0.10				30	21
Industrial/Traffic (MSY)	2.08	1.01	L	7	**	-0.11				56	13

Figure Captions:

Figure 1: Location of the Barcelona (BCN) and Montseny (MSY) measuring stations. Red full circle highlights the location of the BCN measuring station before 2009. Green full circle highlights the new location of the BCN (from 2009) and MSY measuring stations.

Figure 2: Mann-Kendall fit of $PM_{2.5}$ trends at MSY station for the periods 2002-2010 (as in Cusack et al., 2012), 2004 – 2014 (this work), and 2002 – 2014 (largest period available in the time of writing). Reported are: magnitude of the trends [μgm^{-3}/yr]; p-value; Total Reduction (TR) and Residual Component (RC). Significance of the trends following the Mann-Kendall test: *** (p-value < 0.001), ** (p-value < 0.01), * (p-value < 0.05), + (p-value < 0.1).

Figure 3: Mann-Kendall (MK) and Multi-exponential (ME) trends for chemical species at BCN in PM_{10}. Measured concentration (green line); Multi-exponential trend (red line); Multi-exponential residuals (blue line); Mann-Kendall trend (black line); Mann-Kendall residuals (grey line). Trend type: linear (L), single-exponential (SE), double exponential (DE).

Figure 4: Mann-Kendall (MK) and Multi-exponential (ME) trends for chemical species at MSY in PM_{10}. Measured concentration (green line); Multi-exponential trend (red line); Multi-exponential residuals (blue line); Mann-Kendall trend (black line); Mann-Kendall residuals (grey line). Trend type: linear (L), single-exponential (SE), double exponential (DE).

Figure 5: Source contributions from PMF model in PM_{10} at Montseny (MSY) and Barcelona (BCN). Mean values during 2004-2014. Values reported are: ***Source; $\mu g/m^3$; %.***

Figure 6: Mann-Kendall and Multi-exponential trends for source contributions in PM_{10} at BCN. Measured concentration (green line); Multi-exponential trend (red line); Multi-exponential residuals (blue line); Mann-Kendall trend (black line); Mann-Kendall residuals (grey line). Trend type: linear (L), single-exponential (SE), double exponential (DE). Highlighted with yellow colour the source contributions at BCN from *Mineral*, *Traffic* and *Road/work resuspension* were excluded from the trend discussion.

Figure 7: Mann-Kendall and Multi-exponential trends for source contributions in PM_{10} at MSY. Measured concentration (green line); Multi-exponential trend (red line); Multi-exponential residuals (blue line); Mann-Kendall trend (black line); Mann-Kendall residuals (grey line). Trend type: linear (L), single-exponential (SE), double exponential (DE).

Figure 8: Spanish national emission of SO_2 and NO_X (normalized to year 2004).

Figure 9: NASA OMI level 3 tropospheric NO_2 column plotted using the Giovanni online data system, developed and maintained by the NASA GES DISC.

Figure 10: Annual (2004–2014) energy consumption for Spain (normalized to year 2004). Data from the Spanish Ministry of Industry (MINETUR, 2013).

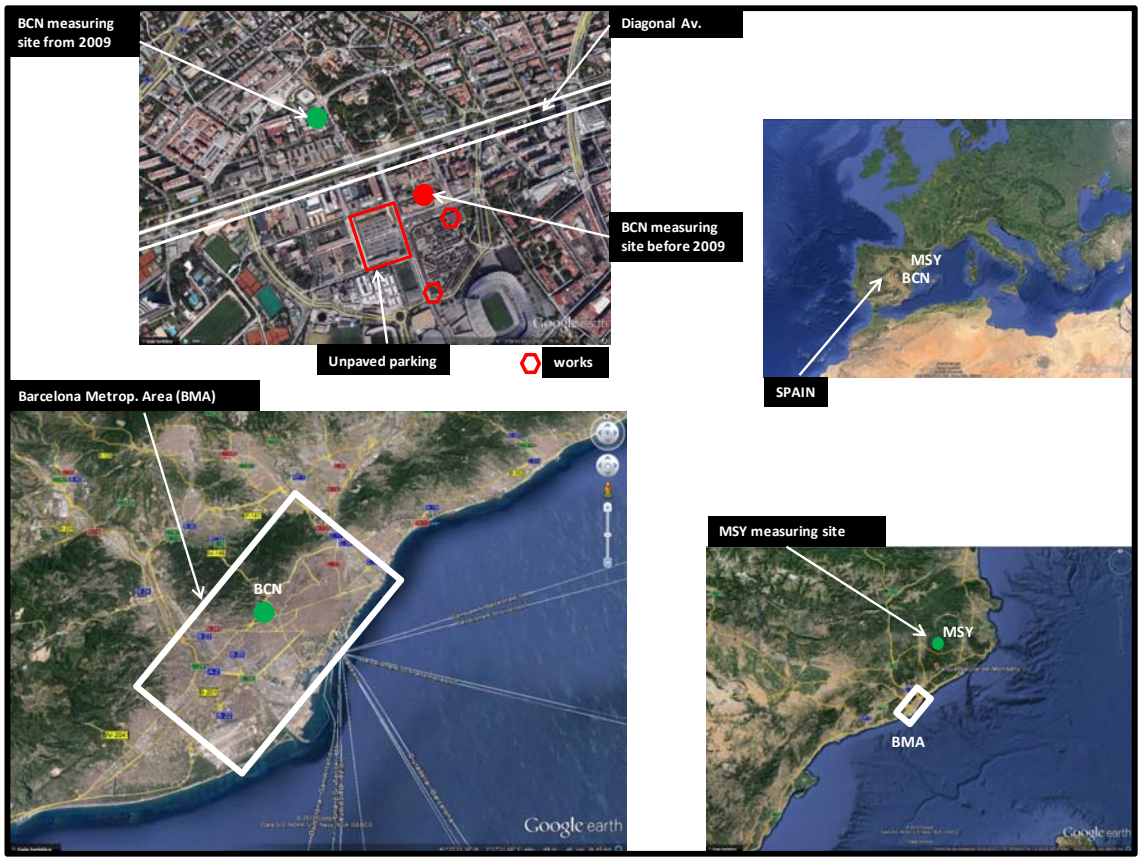

868

869 **Figure 1**

870

871

872

873

874

875

876

877

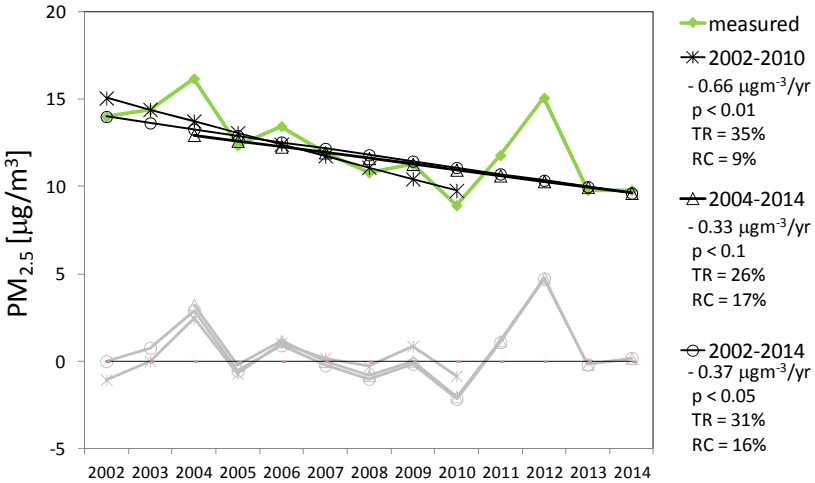

878

879 **Figure 2**

880

881

882

883

884

885

886

887

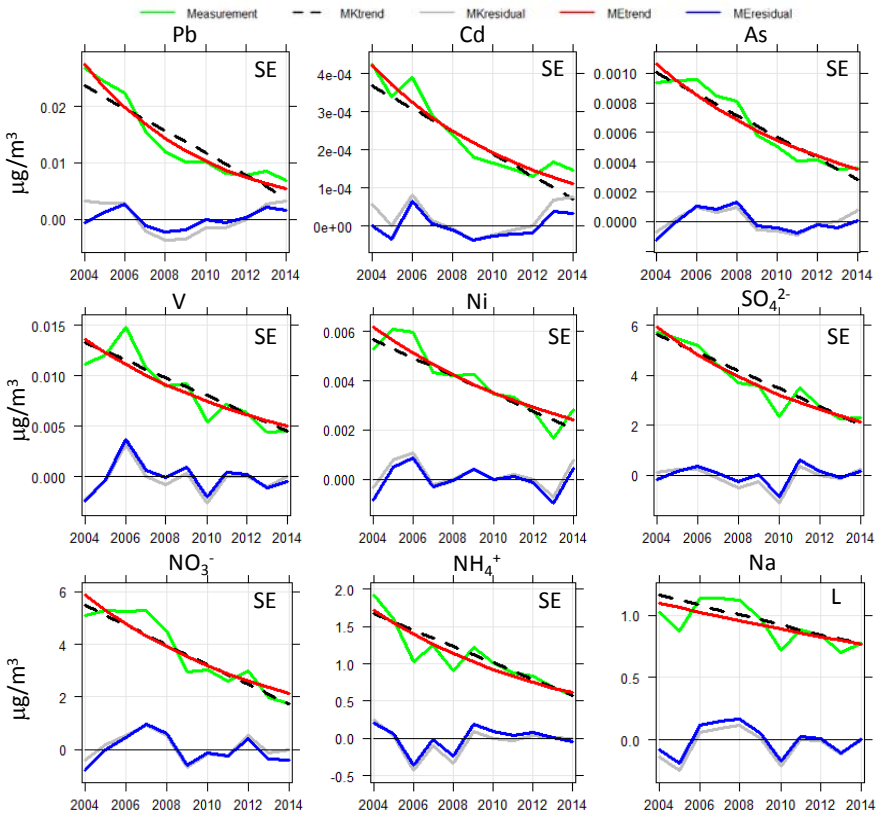
Measurement
MKtrend
MKresidual
METrend
MEresidual
Pb
Cd
As
V
Ni
SO4 2-
NO3 -
NH4 +
Na
SE
L
µg/m3

Figure 3

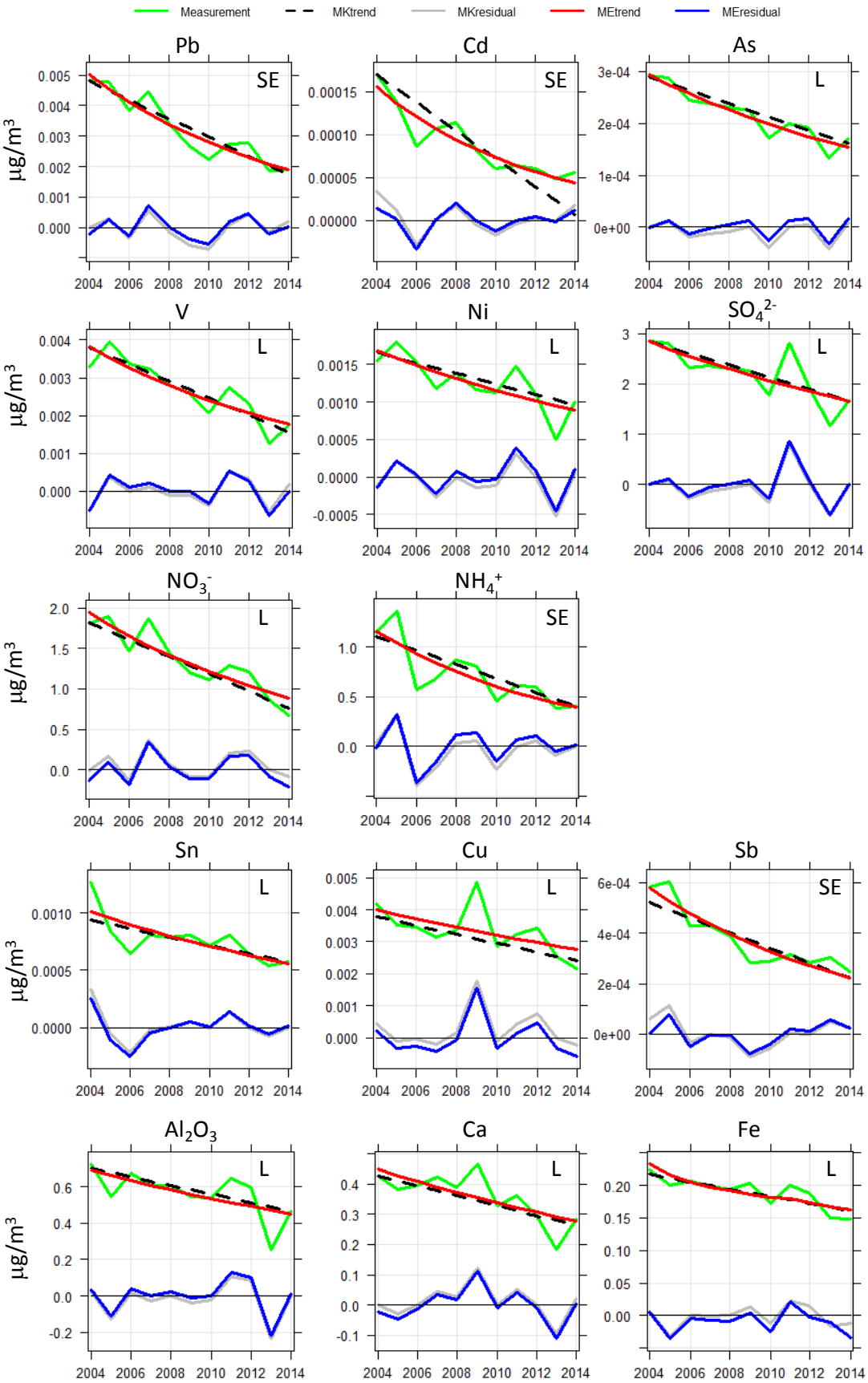
Measurement
MKtrend
MKresidual
METrend
MEresidual
Pb
SE
Cd
SE
As
L
V
L
Ni
L
SO_4^{2-}
L
NO_3^-
L
NH_4^+
SE
Sn
L
Cu
L
Sb
SE
Al_2O_3
L
Ca
L
Fe
L
µg/m³
2004 2006 2008 2010 2012 2014

Figure 4

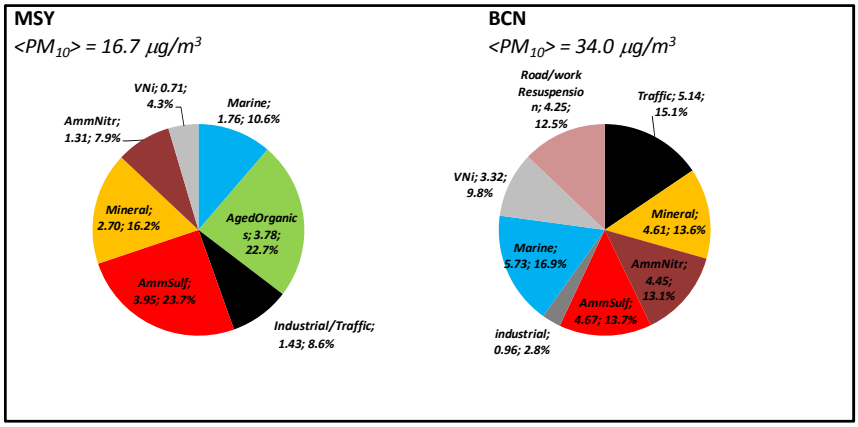
MSY
<PM10> = 16.7 µg/m3
VNi; 0.71; 4.3%
Marine; 1.76; 10.6%
AmmNitr; 1.31; 7.9%
Mineral; 2.70; 16.2%
AgedOrganics; 3.78; 22.7%
AmmSulf; 3.95; 23.7%
Industrial/Traffic; 1.43; 8.6%
BCN
<PM10> = 34.0 µg/m3
Road/work Resuspension; 4.25; 12.5%
Traffic; 5.14; 15.1%
VNi; 3.32; 9.8%
Mineral; 4.61; 13.6%
Marine; 5.73; 16.9%
AmmNitr; 4.45; 13.1%
AmmSulf; 4.67; 13.7%
industrial; 0.96; 2.8%

Figure 5

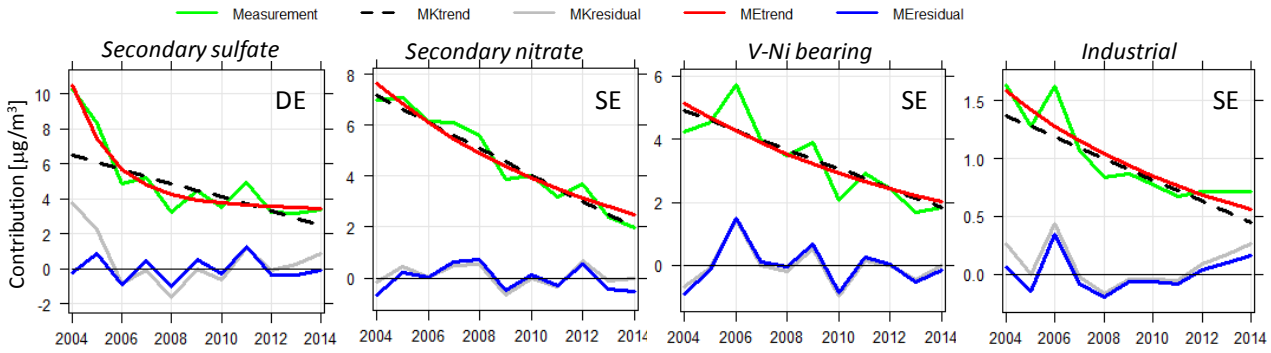

Figure 6

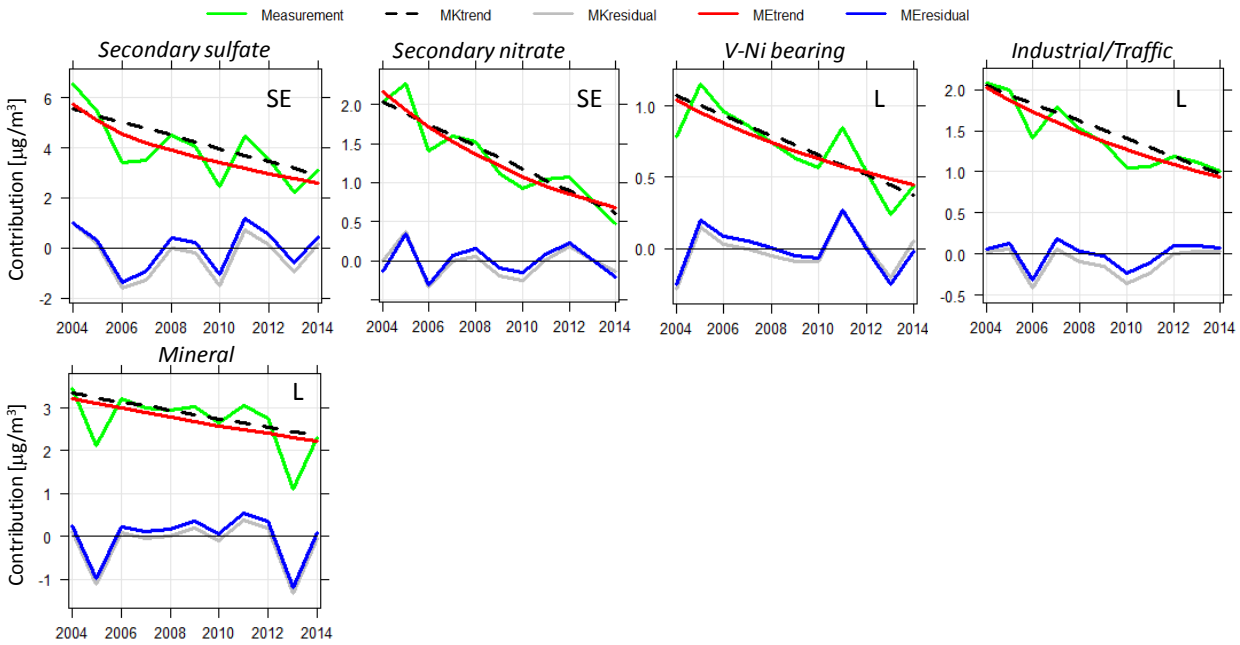

Figure 7

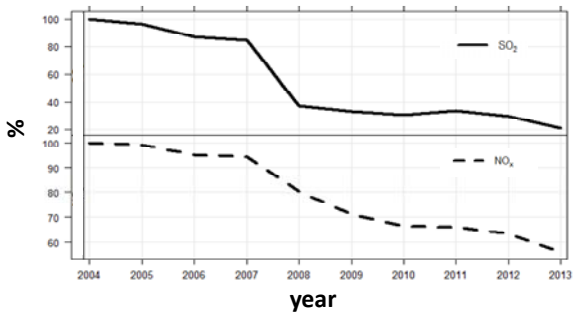

Figure 8

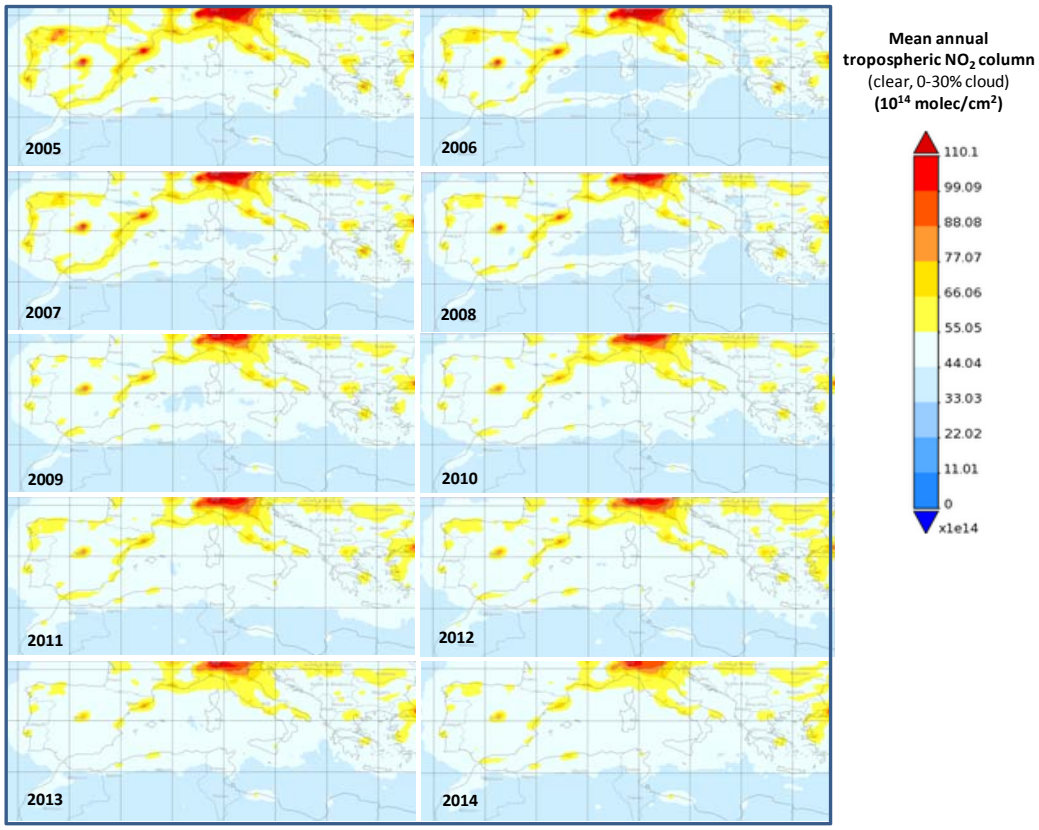

Figure 9

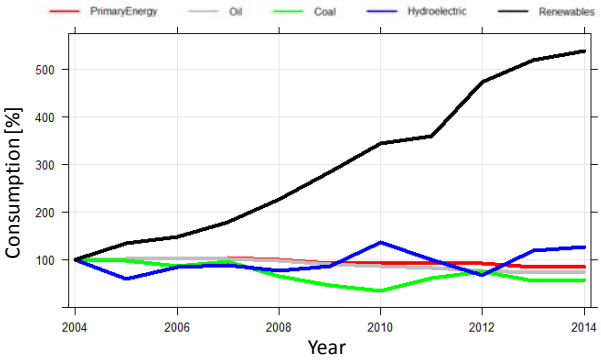

940

941 **Figure 10**

942

943

944

945

946

947

948